



HAL
open science

Biological effects of ultrashort electric pulses in a neuroblastoma cell line: the energy density role

Claudia Consales, Caterina Merla, Barbara Benassi, Tomás Garcia-Sanchez, Adeline Muscat, Franck M. André, Carmela Marino, Lluís Mir

► To cite this version:

Claudia Consales, Caterina Merla, Barbara Benassi, Tomás Garcia-Sanchez, Adeline Muscat, et al.. Biological effects of ultrashort electric pulses in a neuroblastoma cell line: the energy density role. International Journal of Radiation Biology, 2021, 98 (1), pp.109-121. 10.1080/09553002.2022.1998704 . hal-03875108

HAL Id: hal-03875108

<https://hal.science/hal-03875108>

Submitted on 28 Nov 2022

HAL is a multi-disciplinary open access archive for the deposit and dissemination of scientific research documents, whether they are published or not. The documents may come from teaching and research institutions in France or abroad, or from public or private research centers.

L'archive ouverte pluridisciplinaire **HAL**, est destinée au dépôt et à la diffusion de documents scientifiques de niveau recherche, publiés ou non, émanant des établissements d'enseignement et de recherche français ou étrangers, des laboratoires publics ou privés.

Biological effects of ultrashort electric pulses in a Neuroblastoma cell line: the energy density role.

Claudia Consales^{1*#}, Caterina Merla^{1*#}, Barbara Benassi¹, Tomás Garcia-Sanchez^{2,3}, Adeline Muscat², Franck M. André², Carmela Marino¹, Lluís M. Mir^{2#}

*These Authors equally contributed to the work

Claudia Consales <https://orcid.org/0000-0002-7805-4493> email: claudia.consales@enea.it

Caterina Merla <https://orcid.org/0000-0001-8612-9566> email: caterina.merla@enea.it

Lluís M. Mir <https://orcid.org/0000-0002-8671-9467> email: luis.mir@cnrs.fr

Affiliations

¹Division of Health Protection Technologies, ENEA-Italian National Agency for New Technologies, Energy and Sustainable Economic Development, Rome, Italy

² Université Paris-Saclay, Institut Gustave Roussy, CNRS, Metabolic and Systemic aspects of the oncogenesis (METSYS), 94805, Villejuif, France.

³ Department of Information and Communication Technologies, Universitat Pompeu Fabra, Barcelona Spain

Keywords: deposited energy density, extremely low frequency magnetic fields, ultra-short electric pulses, SH-SY5Y, immediate early genes

Abstract

Despite numerous published results describing the biological effects of the exposure to electromagnetic fields (EMFs), the mechanisms of interaction of these fields with biological systems are still a matter of debate, including those associated with exposures to extremely-low-frequency magnetic fields (ELF-MFs), which have been shown to modulate redox homeostasis and to modify the epigenome of SH-SY5Y cells. Here we report an investigation of the accumulated electromagnetic energy density deposited during a 24 hour, 1 mT, 50 Hz exposure contributes to several biological endpoints. We exposed SH-SY5Y cells to the same energy, abruptly deposited by single electric pulses in the range of microseconds or nanoseconds. Under these conditions, we observed no single-pulse-induced changes in reactive oxygen species (ROS) production, miR-34b/c expression, or the appearance of indicators of apoptosis. We then asked whether the electric field induced during the 24 and 48 hour has a significant effect when delivered directly, without the magnetic field. No ROS formation in cells exposed for 24 or 48 hours to an electric field of the same amplitude as the one induced by 1mT sinusoidal (50Hz) MF.

Finally, we characterized SH-SY5Y response to single microsecond and nanosecond electric pulses at increasing levels of deposited energy density (DED). We observed *egr-1* and *c-fos* significant activation independently of the cell electroporation threshold and cell fusion at the highest electric pulse intensity.

These results contribute to a deeper comprehension of the molecular effects induced on SH-SY5Y cells by microsecond and nanosecond electric pulses.

Abbreviations

EMF: ElectroMagnetic Field

ELF-MF: Extremely Low Frequency Magnetic Field

MF: Magnetic Field
1 MPP⁺: 1-methyl-4-phenylpyridinium
2
3 ECT: ElectroChemoTherapy
4 EGT: ElectroGeneTherapy
5
6 DED: Deposited Energy Density
7
8 EDTA: EthyleneDiamine-Tetra-Acetic acid
9
10 BSA: Bovine Serum Albumin
11
12 DMSO: dimethyl sulfoxide (DMSO)
13
14 PI: Propidium Iodide
15
16 DHE: DiHydroEthidium
17
18 H2-DCFDA: 2',7'-DiChloroDihydrofluorescein DiAcetate
19
20 DMEM/F12: Dulbecco's Modified Eagles Medium/Ham's F12
21
22 IARC: International Agency for Research on Cancer
23
24 PDMS: PolyDiMethylSiloxane
25
26 PBS: Phosphate-Buffered Saline
27
28 ROS: reactive oxygen species
29
30 μ s: microsecond
31
32 ns: nanosecond
33
34 miRNA: microRNA
35
36 MFI: Mean Fluorescence Intensity
37
38 Egr-1: Early Growth Response 1
39
40 TMP: TransMembrane Potential
41
42
43
44
45
46
47
48
49
50
51
52
53
54
55
56
57
58
59
60
61
62
63
64
65

1. Introduction

There is wide interest in understanding electromagnetic field (EMF) effects in biology, both to enable a better comprehension of the interaction mechanisms for protection purposes of the exposed populations, and to establish innovative and advantageous medical treatments [1, 2]. A large number of studies, applying very different exposure modalities in terms of amplitudes, waveforms and frequencies (from direct current, up to tens of GHz) have been carried out in many experimental models, both *in vitro* and *in vivo*, experimental models, with a wide range of different outcomes. Most of these studies suffer of the lack of a well-characterized mechanisms of interaction for the observed effects [3, 4, 5, 6].

In the bio-electromagnetics research community, considerable attention is devoted to the extremely low frequency (ELF) electric and magnetic fields, due to their widespread distribution in everyday life (e.g. electrical utility power lines, house hold appliances, etc.) and to their use in approved medical treatments, in particular for brain stimulation (e.g. Transcranial Magnetic Stimulation and Deep Brain Stimulation). The therapeutic efficacy of these latter procedures is limited by the lack of knowledge of a clear action mechanism and effector pathways, at the molecular level and at the level of cells and tissues [6- 8].

Several studies, aiming at understanding the effect of ELF-magnetic fields (ELF-MFs) on the nervous system, identified cell redox homeostasis as one of the exposure targets [6, 9-11]. We have extensively characterized the response of neuronal-like cells (SH-SY5Y, human neuroblastoma cell line) to 50Hz, 1mT sinusoidal magnetic flux

1 density (B), providing evidence of effects on the cellular redox system and epigenome [10-12]. Indeed, we
2 demonstrated that a 50 Hz, 1 mT MF, over 72 hours of continuous exposure, alters redox homeostasis by inducing an
3 increase of ROS with subsequent protein carbonylation, which sensitizes cells to the neurotoxin 1-methyl-4-
4 phenylpyridinium (MPP⁺) [10]. We demonstrated further that the same MF exposure (50 Hz, 1 mT, up to 72 hours)
5 downregulates the expression of microRNA-34b/c in SH-SY5Y cells and in mouse primary neurons by hyper-
6 methylating the miR promoter [12]. MicroRNA are short, non-coding and endogenously expressed RNA that play a
7 pivotal role in post transcriptional regulation of gene expression [13]. miR-34b and miR-34c are targets of p53 and are
8 involved in physiological cell differentiation by regulating the cell cycle and apoptosis [14, 15]. Considering the pivotal
9 role that these microRNAs play in normal cell homeostasis, it is not surprising that their action is often mis-regulated in
10 pathological processes. In particular, miR-34b/c expression is downregulated in cancer and neurodegenerative diseases
11 [16].

12 In addition to these studies oriented toward risks evaluation and individuals protection, another area of active
13 research involves the application of ultra-short (from millisecond down to hundreds of picoseconds) and intense (from
14 few kV/m up to tens of MV/m) electric pulses to cells and tissues. In the clinic today already we find therapeutic
15 procedures that use microsecond electric pulses with fields up to 100 kV/m -electrochemotherapy (ECT) [17, 18],
16 electrogenetherapy (EGT) [19], and irreversible electroporation (IRE) [20]. Nanosecond-pulses-based medical
17 application, with field greater than 1 MV/m, include nerve and muscle stimulation [21] and new oncologic treatments
18 [22].

19 For these high field amplitude exposure conditions (microsecond and nanosecond electric pulses), the primary effect
20 on cells is believed to be permeabilization of cell membranes. The pulsed external field induces a large voltage across
21 the plasma membrane, and this causes the formation of conductive lipid pores (electroporation). Under the right
22 conditions this is followed by a persistent permeabilization that results from structural and chemical rearrangements of
23 membrane constituents and other membrane-associated species (electropermeabilization) [23, 24]. This breakdown of
24 the membrane barrier function triggers a set of secondary events, such as cell apoptosis -with or without caspase
25 activation- [25, 26], promotion of intracellular calcium oscillations [27, 28], alteration of ion conductance through the
26 membrane [29, 30], cytoskeleton rearrangements, with concomitant cell blebbing and fusion [31], and reactive oxygen
27 species production [32, 33]. Nanosecond electric pulses with amplitudes under the electroporation threshold may also
28 affect ion channels gating, which would enable electromodulation of cell physiology without porating damage to the
29 cell membrane. For example, by activating voltage-gated sodium channels, low-field electric pulses could induce action
30 potential generation. [21].

31 Despite increasing evidence on the effects on cells physiology exerted by nanosecond and microsecond electric
32 pulses that do not cause cell electroporation, the molecular pathways activated by such stimulations have not yet been
33 extensively investigated and are still poorly understood.

34 Hence, in the study reported in this article, we pursued different objectives. First, we compared the biological effects
35 triggered by nanosecond and microsecond electric pulses in SH-SY5Y human neuroblastoma cells to those elicited by a
36 chronic sinusoidal 50 Hz exposure. Applied electric pulse parameters were selected to deposit the same energy density
37 than the one cumulated during a 24 and 48 hours, 50 Hz, 1 mT, MF exposure [10, 11, 12]. In this way, we aimed at
38 clarifying the role of the Deposited Energy Density (DED) in the induction of redox modulation, cell death and
39 epigenetic regulation (miR-34b/c expression) for very different exposure durations.

1 Second, to further characterize the molecular responses to EMF exposure, we investigated the role elicited by the
2 magnetic component of the exposure versus the electric one. This study was carried out by exposing SH-SY5Y cells to
3 an electric field of the same amplitude as that induced by the 50 Hz, 1mT MF.

4 Finally, we characterized SH-SY5Y cells responses to a single microsecond or nanosecond electric pulse with
5 increasing levels of DED. In other published analyses of electric pulse effects, different DEDs were applied, different
6 effects were observed, and scaling rules were proposed based on the magnitude of a given endpoint (e.g. electroporation
7 achievement) [34-38]. Here, we use DED as a normalizing physical quantity to enable the comparisons among different
8 electromagnetic exposures.
9

10 This study provides a first description of different biological effects in the same cell type produced by different
11 exposure modalities with comparable energies, which we expect will lead to a better understanding of the mechanisms
12 underlying the response of biological systems to magnetic and electric stimulation.
13
14
15
16
17
18
19
20
21
22
23
24
25
26
27
28
29
30
31
32
33
34
35
36
37
38
39
40
41
42
43
44
45
46
47
48
49
50
51
52
53
54
55
56
57
58
59
60
61
62
63
64
65

2. Materials and methods

2.1. Chemicals

Culture media, serum and supplements, trypsin-EDTA, were obtained from Gibco (Paris, France). Bovine serum albumin (BSA), dimethyl sulfoxide (DMSO), ethylenediamine-tetra-acetic acid (EDTA), MPP⁺, Propidium Iodide (PI), RNase A, Trypan blue solution (0.4%) and Triton X-100 were purchased from SIGMA-Aldrich (St Louis, MO, USA). The fluorescent probes dihydroethidium (hydroethidine, DHE) and 20,70-dichlorofluorescein diacetate (H2-DCFDA) were obtained from Molecular Probes (Thermo Fisher Scientific, Waltham, MA, USA).

2.2. Exposure systems

To make a comparison, in terms of effects, between the exposures performed with the magnetic field (1 mT, 50 Hz exposure lasting 24 hour) and the electric pulses, the pulse characteristics were chosen in order to have a deposited total energy density identical to the energy density (around 0.015 J/m³) deposited in the medium during the long magnetic field exposures applied to the same cells in our previous experiments [10-12]. The electromagnetic energy density deposit (J/m³) in the medium containing the cell monolayer was computed by equation (1)

$$DED = \sigma\tau E^2, \quad (1)$$

where σ is the conductivity of the cell culture medium equal to 1.5 S/m and τ represents the duration of the exposure expressed in seconds. For the magnetic field stimulation τ was equal to 24 hour (86400 s) while it was 100 μ s or 10 ns for the electric pulses exposures.

The electric field indicated with E (eq. 1) is the one induced by the magnetic stimulation and computed by numerical simulations (Comsol Multiphysics v. 5) in the actual experimental conditions as already described in [10]. The induced electric field amplitude in the cell monolayer (at the bottom of the Petri dish) was 0.3 mV/m (peak value) with an homogeneity larger than 95%. The electric field intensity required when electric pulses were applied was computed with equation (1), as in this case we decided that the total DED should have the same value as the one deposited by the magnetic stimulation. Electric pulses of higher energies were also used in order to globally evaluate the cell responses in a dose dependent manner. The whole set of stimulation parameters is listed in Table 1.

| Conditions | Applied Voltage (V) | DED (J/m ³) | E field (V/cm) |
|---------------------|---------------------|------------------------------|----------------|
| 1 pulse 100 μ s | 0.1 | 0.015 | 0.1 |
| 1 pulse 100 μ s | 10 | 150 | 10 |
| 1 pulse 100 μ s | 600 | 54000 | 600 |
| 1 pulse 100 μ s | 1000 | 1.5 \times 10 ⁶ | 1000 |
| 1 pulse 10 ns | 10 | 0.015 | 10 |
| 1 pulse 10 ns | 1000 | 150 | 1000 |

Table 1 The whole set of stimulation conditions for microsecond and nanosecond pulsed electric fields.

Adherent SH-SY5Y cells were exposed in 6-cm Petri dishes, where a pair of stainless-steel electrodes (1 mm thick each) were placed parallel at a distance of 1 cm from each other (Fig. 1 panel A), Polydimethylsiloxane (PDMS) holders were fabricated (to get an exposure volume of 5 \times 1 \times 0.5 cm³) and included in the Petri dishes. They served to

accurately maintain the chosen electrode distance and the electrodes parallelism in order to assure controlled exposure conditions. In Fig. 1A, the fabricated PDMS holders are presented together with photos of the Petri dishes with the metallic electrodes placed into the PDMS spacers for the microsecond and nanosecond pulses exposures. The metallic electrodes were connected to a Cliniporator (IGEA, Carpi, Italy) pulse generator to deliver microsecond pulses (duration of 100 μ s, rise/fall times 10 μ s) of amplitudes equal to 1000 and 600 V. A Tektronix generator (AFG3251) was used to deliver microsecond pulses (duration of 100 μ s) with the lowest amplitudes (10 and 0.1 V). A FID Technology generator (model, FID GmbH, Burbach, Germany) was used to deliver nanosecond pulses (duration of 10 ns, rise/fall time of 1 ns) of 1000 V or 10 V. When nanosecond pulses of 10 V were applied to cells an external high voltage attenuator 245NMFFP-100 Barth Electronics (with a linear attenuation factor of 100) was included in the pulse delivery line between the pulse generator and the exposure device. In Fig. 1 B, examples of signal waveforms delivered to cells are presented to demonstrate the absence of artifacts and spurious reflections. These representative examples of the delivered waveforms demonstrate the suitable matching of the generators to the biological load. This aspect was especially relevant when 10 ns electric pulses were applied to SH-SY5Y cells. In this case, a precise volume (1.3 mL) of culture medium was pulsed during the experiments (height of culture medium of 1.3 mm) to suitably match the impedance of the biological load to the 50 ohm corresponding to the output impedance of the pulse generators. Thus matching was obtained thanks to the choice of the height of the biological solution enclosed between the electrodes, avoiding the use of specific low conductive buffers usually needed to match the biological load at 50 ohm [39, 40].

In order to separately study the effects of the application of a continuous electric field equivalent to the one induced by the 1mT sinusoidal (50 Hz) magnetic field in the samples, sinusoidal 50 Hz electric field of very low intensity was directly applied to cells (Fig. 1 C). The setup consisted in a voltage divider (1:1000) made with a precision decade divider (Vishay, CNS 471) and an operational amplifier connected to a waveform generator (Agilent 33250A). According to the estimations obtained in the electromagnetic simulations [10, 11], two different 50 Hz electric fields with amplitudes E_{peak} of 0.6 mV/m and 0.3 mV/m were applied, respectively, for 24 or 48 hours, using stainless steel parallel plate electrodes. A PDMS insert was placed in the Petri dishes to ensure the correct positioning of the electrodes, as schematically shown in the left panel of Fig. 1C. In the central panel a picture of the exposure setup for such kind of signals is also reported as well as the corresponding waveform (right panel).

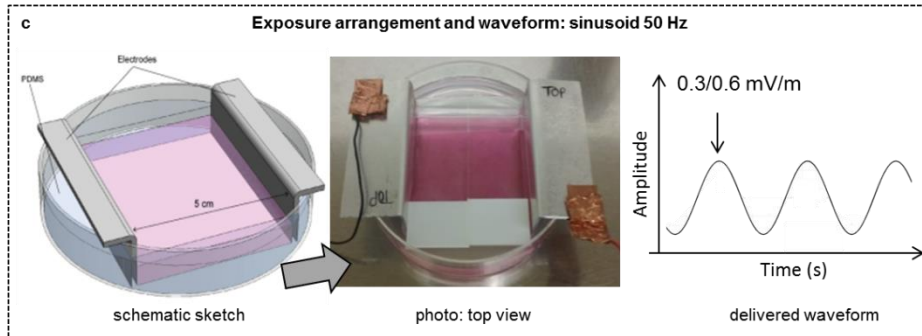
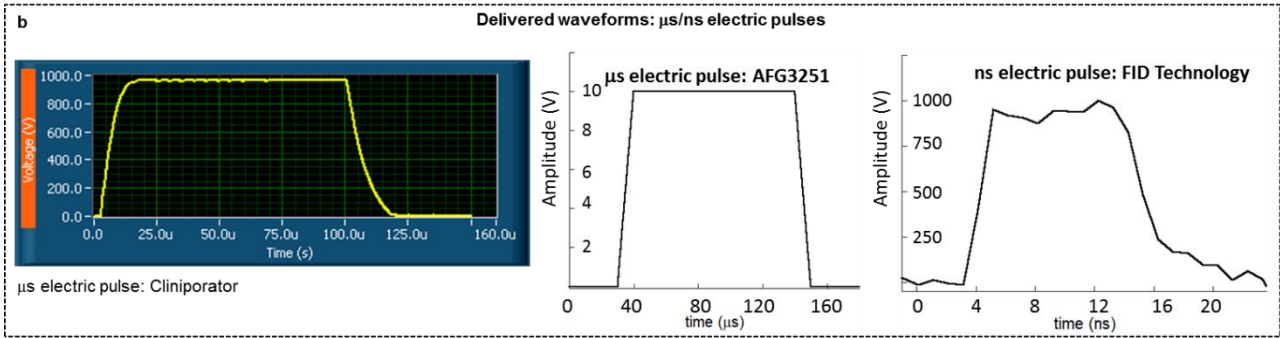
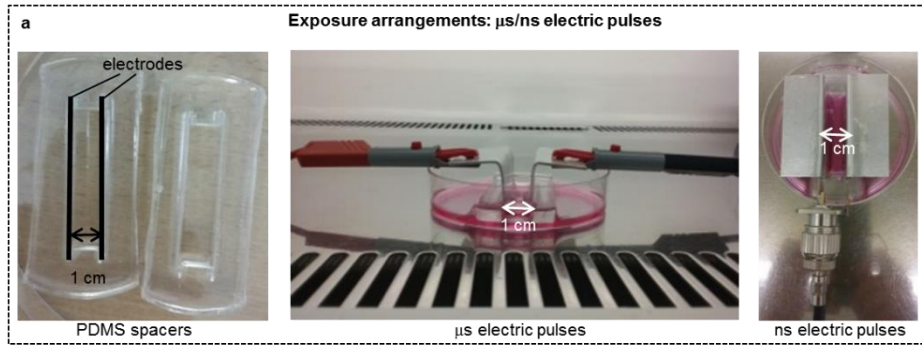


Fig. 1: a) PDMS spacers, left, and picture of the exposure arrangements for microsecond (center) and nanosecond (right) pulses delivery. b) Delivered waveforms for microsecond (left and central panels) and nanosecond pulses (right panel). Figures reporting the maximum delivered voltages are reported as examples. c) Exposure arrangement and waveform of the 50 Hz sinusoidal electric field

2.3. Cell culture and exposure

Human SH-SY5Y neuroblastoma cells were purchased from the European Collection of Cell Culture, cultured in complete Dulbecco's modified Eagles medium/Ham's F12 (DMEM/F12, 50:50 mix, Gibco), supplemented with 10 % heat-inactivated fetal bovine serum, 2 mM L-glutamine, 100 $\mu\text{g}/\text{ml}$ penicillin-streptomycin, and used before the fifteenth culture passage. The cells were maintained at 37°C in a 5% CO_2 atmosphere in air, routinely trypsinized and plated at $4 \times 10^4/\text{cm}^2$ in flasks. Cell viability was assessed by Trypan blue dye exclusion.

Two days before pulsed electric field stimulation, 3×10^5 cells were plated inside the Polydimethylsiloxane (PDMS) insert. After stimulation, cells were harvested, according to the specific biological experiment to be carried out; in any case, they were maintained in culture for no longer than 48 hours. For each experiment and for each experimental condition, sham samples were prepared by plating the cells in the same and electrodes were placed in the PDMS insert

1 to mimic the exposure as in the exposed samples (at the same temperature and for the same time), but no electric
2 stimulation was applied.

3 For continuous exposure to sinusoidal electric field, 8×10^5 cells were plated 48 hours before the beginning of the
4 exposure, and ROS were evaluated 24 and 48 hours after the beginning of the exposure.
5

6 7 *2.4. Cell morphology analysis* 8 9

10 Cells were seeded on coverslips put inside PDMS insert two days before the stimulation. Twenty-four hour after the
11 electric field stimulation, culture medium was removed and, after one wash with PBS, cells were fixed for 20 minutes
12 with 4% paraformaldehyde (Sigma) and rinsed with PBS. Just after the washing, cells were incubated for 30 min with
13 wheat germ agglutinin (Alexa Fluor 488 Thermo Fisher, 1:300) to stain the plasma membranes. After PBS wash, cells
14 were permeabilized with 0.1 % Triton X100 (Sigma) for 5 min, washed with PBS, and incubated for 30 min with Alexa
15 Fluor 568 Phalloidin (1:500, Thermo Fisher Scientific). After several washings with PBS, a mounting solution
16 containing DAPI (Vectashield, Vector Laboratories, USA) was applied to the slides to stain nuclear RNA/DNA, and the
17 slides stored at 4 °C until images acquisition was performed using a confocal microscope (Leica Microsystem SP8).
18
19
20
21
22

23 24 *2.5. Flow-cytometric analysis of ROS generation* 25 26

27 Flow-cytometry analyses were performed using a C6 flow cytometer (BD Accuri, Becton Dickinson). Forward (FSC-H)
28 and side (SSC-H) scatterings were used to exclude cellular debris from the analysis and to gate the intact/healthy cells.
29 To quantify the oxidative stress, cells were stained with either DHE (detection of superoxide radicals) or H₂-DCFDA
30 (measurement of H₂O₂) [10, 11]. Cells were harvested on ice, washed twice in cold PBS, and re-suspended in 5 μM
31 DHE in PBS for 20 min at 37 °C in the dark, or in 5 μM H₂-DCFDA in PBS for 20 min at 37 °C in the dark. After a
32 final wash in PBS, cells were immediately transferred into a tube kept on ice until the flow cytofluorometric analysis. In
33 each measurement, a minimum of 10.000 cells were analyzed. Data were acquired and analyzed using the BD Accuri
34 C6 software (Becton Dickinson). For fluorescence data analysis, the mean fluorescence intensity (MFI) was calculated
35 for each sample as the mean fluorescence value in the channel of the probe-labelled cells minus the mean fluorescence
36 value of unstained cells.
37
38
39
40
41
42
43

44 *2.6. Assessment of cell permeabilization* 45 46

47 Cell permeabilization was assessed by fluorescent microscopy. The treated SH-SY5Y cells were trypsinized and re-
48 suspended in DMEM, and then Yo-Pro-1 (Life Technologies) was added, at a final concentration of 3 μM, 5 minutes
49 before the acquisition of the first image. To test cell permeabilization we delivered different pulse protocols consisting
50 in 1 (Table 1) or in 8 electric pulses of 100 μs duration, at a repetition rate of 1 Hz, with field amplitude of 600 or 1000
51 V/cm respectively.
52

53 Images were acquired at $\lambda = 510$ nm using an inverted microscope (AxioVert 100, Zeiss) with an exposure time of 300
54 ms using a 10× objective). Three independent experiments were performed for each tested condition.
55
56
57
58

59 *2.7. Western Blotting* 60 61 62 63 64 65

Cells were re-suspended in lysis buffer containing 50 mM Tris- HCl (pH 8.0), 150 mM NaCl, 1 % NP-40, and 12 mM Na-deoxycholate (Sigma) supplemented with protease and phosphatase inhibitors cocktail (Merck, Germany). Lysates were centrifuged at 13,000 rpm for 10 min at 4 °C to discard cellular debris. Protein concentration was determined by the Lowry protein assay (Bio-Rad Laboratories, Hercules, CA, USA). Proteins were separated by SDS-PAGE and transferred to 0.2 µm nitrocellulose membranes (GE Healthcare Life Science, Europe) that were probed with anti-PARP1 (Cell signaling, 1:1500) and anti-beta actin (Santa Cruz, 1:2000) antibodies. After immuno-staining with appropriate secondary horseradish peroxidase-conjugated goat anti-rabbit or anti-mouse antibodies (SIGMA), bands were revealed using a Fluorchem Imaging system (Alpha Innotech, San Leandro, CA, USA) and the Amersham ECL detection system (GE Healthcare Life Science), and then quantified by densitometry. As positive control for apoptosis detection by immunostaining, the proteins extracted from cells exposed for 48 hours to etoposide (VP-16) at a final concentration of 5 µM were included in all the gels together with the experimental samples.

2.8. MicroRNA Expression Analysis

Analysis of mature miRNA expression was carried out on total RNA extracted with the miRcury RNA isolation kit (Exiqon). Ten nanograms of total RNA were retro-transcribed by the miRcury LNA universal RT microRNA kit (Exiqon) and the cDNA diluted 1:80 and amplified by the miRcury LNA SYBR green master mix and miR-specific LNA PCR primer sets (Exiqon), according to manufacturer's instructions. All reactions were run in quadruplicate and the relative abundance of each specific miR (34b, and 34c) was normalized to small nucleolar RNA (U6) by applying the $2^{-\Delta\Delta C_t}$ method [41]. Three independent experiments were performed for each tested condition.

2.9. Genes expression

Total RNA was extracted with the miRcury RNA isolation kit (Exiqon). The amount and purity of the extracted RNA was evaluated using an optic fiber spectrophotometer (Nanodrop ND-1000, NanoDrop Technologies, Wilmington, DE, USA) calculating the 230/260 nm and 260/280 nm absorbance ratios. Five hundred nanograms of total RNA were retro-transcribed with random primers into total cDNA by TaqMan® Reverse Transcription Reagent (Applied Biosystems, Thermo Fisher Scientific), according to manufacturer's indications. Analysis of the genes expression was carried out with 1 µL of cDNA using SYBR Green master mix (Thermo Fisher) and a 7500 Real-Time PCR System (Thermo Fisher Scientific). PCR conditions were as follows: 45 cycles at 95 °C for 30 s and 60 °C for 30 s.

All reactions were run in triplicate and the relative abundance of the specific mRNA levels was calculated by normalizing to the 18S rRNA expression using the $2^{-\Delta\Delta C_t}$ method [41]. Three independent experiments were performed for each tested condition.

The complete list of and the used primer sequences is displayed in Table 2.

| | | |
|-------|---------|------------------------------|
| egr-1 | Forward | 5'-CAGCAGCCTTCGCTAACC-3' |
| | Reverse | 5'- CCACTGGGCAAGCGTAA-3' |
| c-fos | Forward | 5'-TACTACCACTCACCCGCAGACT-3' |
| | Reverse | 5'-GAATGAAGTTGGCACTGGAGAC-3' |

| | | |
|-----|---------|-------------------------------|
| 18S | Forward | 5'-GGCCCTGTAATTGGAATGAGTC-3' |
| | Reverse | 3'-CCAAGATCCAACACTACGAGCTT-3' |

Table 2 Sequences of the primers used to study gene expression

2.10. Statistical analysis

The variations of the samples values are reported as mean \pm S.D. calculated with $n \geq 3$ replicates. After assessing the normal distribution of our results from sham and stimulated samples by using the Shapiro-Wilk and Shapiro-Francia normality tests implemented in Matlab (2016a, the Math Works, USA), the significance of nanosecond and microsecond electric pulse stimulation was evaluated using the Student's T test, where the null hypothesis was that there is no significant difference between the means of the two data sets. We used the KaledaGraph program (Synergy Software, Reading PA, USA) by applying the two-sided Student's t test. The precise number of experimental replicates, as well as the experimental groups that have been compared and statistically analyzed, have been detailed in the previous paragraphs. p values < 0.05 were considered statistically significant and indicated as follows: * $p < 0.05$; ** $p < 0.01$; *** $p < 0.001$.

3. Results

3.1. Ineffective DED role in inducing cell redox impairment, cell apoptosis, and miR-34b/c modulation

SH-SY5Y neuroblastoma cells were exposed either to a single 100 μ s pulse of 0.1 V (induced electric field in the sample: 0.1 V/cm; DED: 0.015 J/m³) or to a single 10 ns pulse of 10 V (induced electric field in the sample 10 V/cm; DED: 0.015 J/m³). ROS generation was analyzed just after the electric pulse delivery (T0) and at three different time points: 1 hour, 6 hours and 24 hour (respectively T1, T6, T24). ROS were also evaluated in non-pulsed control samples. The absence of detectable hydrogen peroxide production (fluorescence from H₂-DCFDA) indicated that neither the microsecond electric pulse nor the nanosecond electric pulse exposure induced changes in ROS generation, at any considered time point (Fig. 2A, D).

To verify whether the delivery of the nanosecond and/or microsecond electric pulses, as described above, might induce apoptosis in SH-SY5Y cells, PARP-1 cleavage was assessed 24 and 48 hours after the pulse delivery. As shown in Fig. 2B and 2E, neither the 100 μ s at 0.1 V/cm nor the 10 ns at 10 V/cm pulses triggered an apoptotic process, which was clearly activated in the included positive controls (etoposide administration for 24 or 48 hours).

To evaluate the effect of the applied electric pulses on miRNA-34b and miRNA-34c, their expression level was assessed at 1, 6 and 24 hour after the pulse delivery. At all the time points analyzed, no significant variation was detected in the microRNAs expression (Fig. 2C, F).

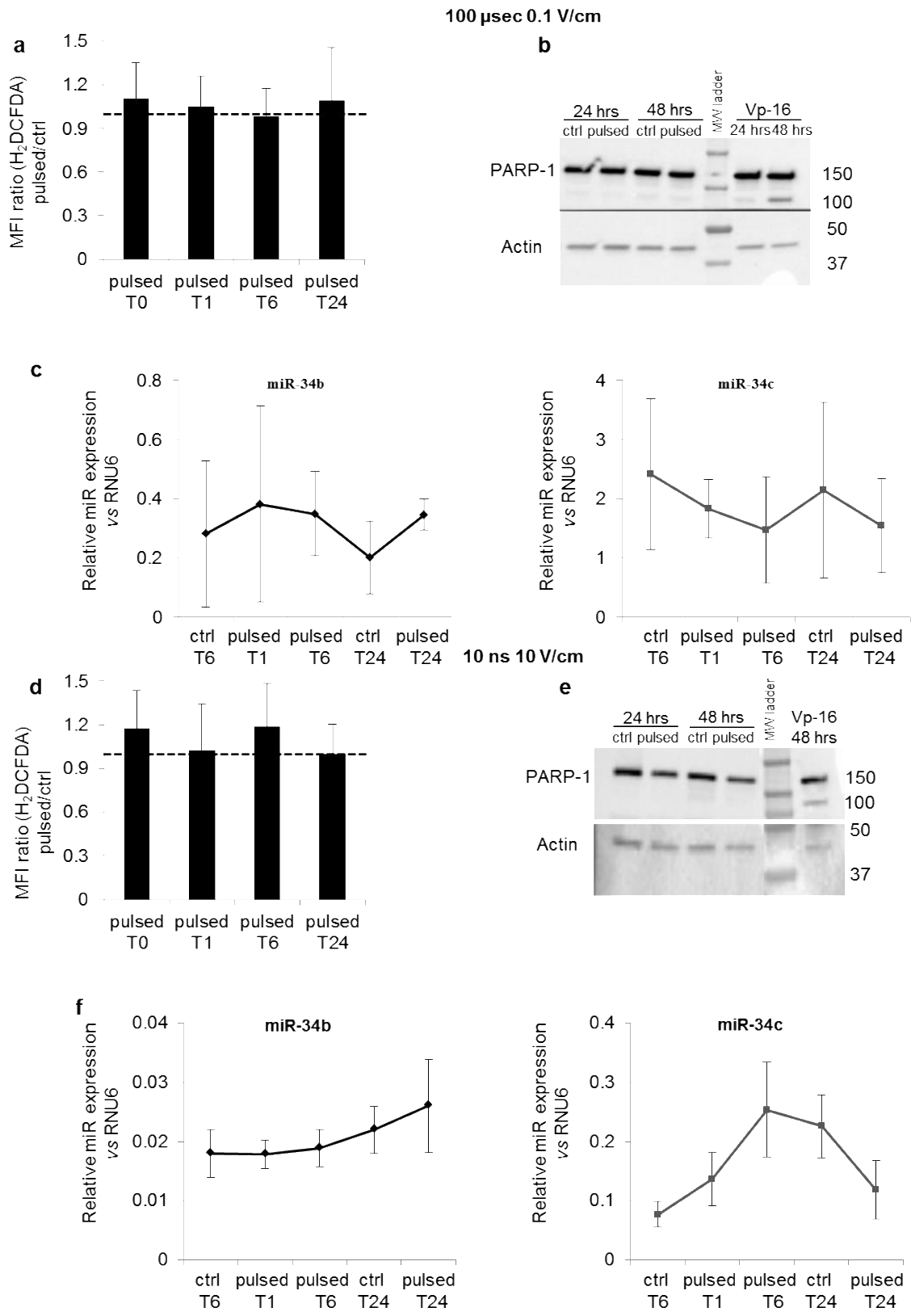


Fig. 2 A) and D) ROS assessment, B) and E) apoptosis evaluation, C) and F) miR 34-b/c expression in SH-SY5Y cells after their pulsation with the same energy density, using one pulse of 100 μ s at 0.1 V/cm (A, B and C) or one pulse of 10 ns at 10V/cm (D, E and F). ROS data are expressed as relative mean fluorescence intensity (MFI), while the expression of miRNA-34 b/c is related to the standard U6. The dashed line corresponds to a fold change of 1

3.2. 50 Hz sinusoidal electric stimulation does not alter SH-SY5Y cells redox homeostasis

As described in [10], 50 Hz, 1mT MF exposure altered SH-SY5Y redox balance by increasing ROS production and proteins carbonylation. To verify whether this redox effect might be related to the electric field component (induced by the 50 Hz, 1mT MF exposure), SH-SY5Y cells were exposed up to 48 hours to a sinusoidal electric field of 0.3mV/m, an intensity equivalent to that induced by the 50 Hz, 1mT MF exposure. The intensity of the induced electric field in the cell monolayer was numerically computed and fully described in [10], as also reported in the Materials and Methods section. Cells were also exposed to a higher electric field 0.6 mV/m.

ROS production was evaluated at 24 and 48 hours post exposure, and no increase in ROS production was detected at either time points (Fig. 3) for an electric field intensity of 0.3 mV/m. Similar results were obtained for the higher electric field intensity (data not shown).

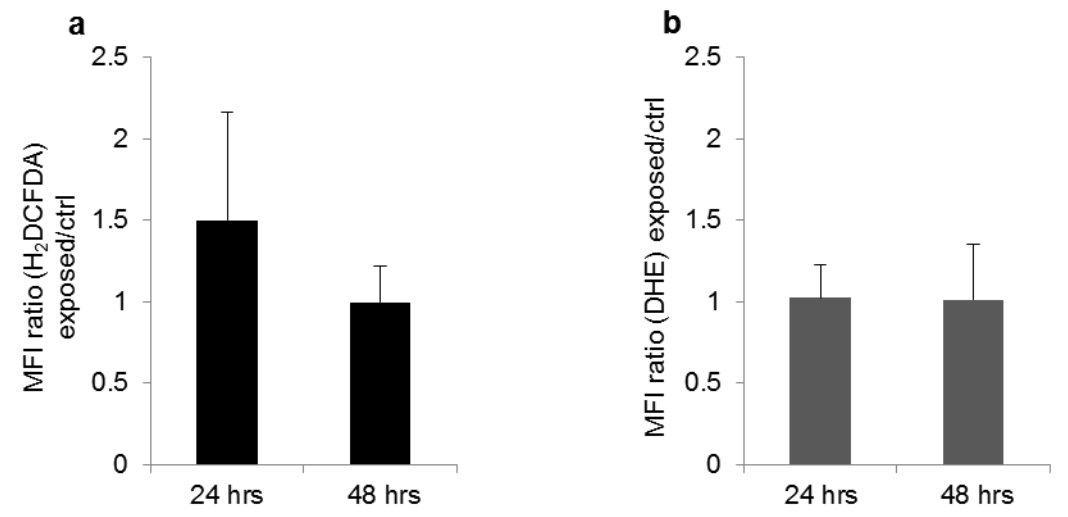


Fig. 3 ROS assessment in SH-SY5Y cells exposed to a 0.3 mV/m sinusoidal (50Hz) electric field. ROS production was evaluated after 24 and 48 hours of exposure through the determination of the levels of A) H₂O₂ (using H₂DCFDA) or B) superoxide (using DHE) as detailed in the Materials and Methods. Data are expressed as relative mean fluorescence intensity (MFI). Values are the means \pm S.D. of three independent experiments

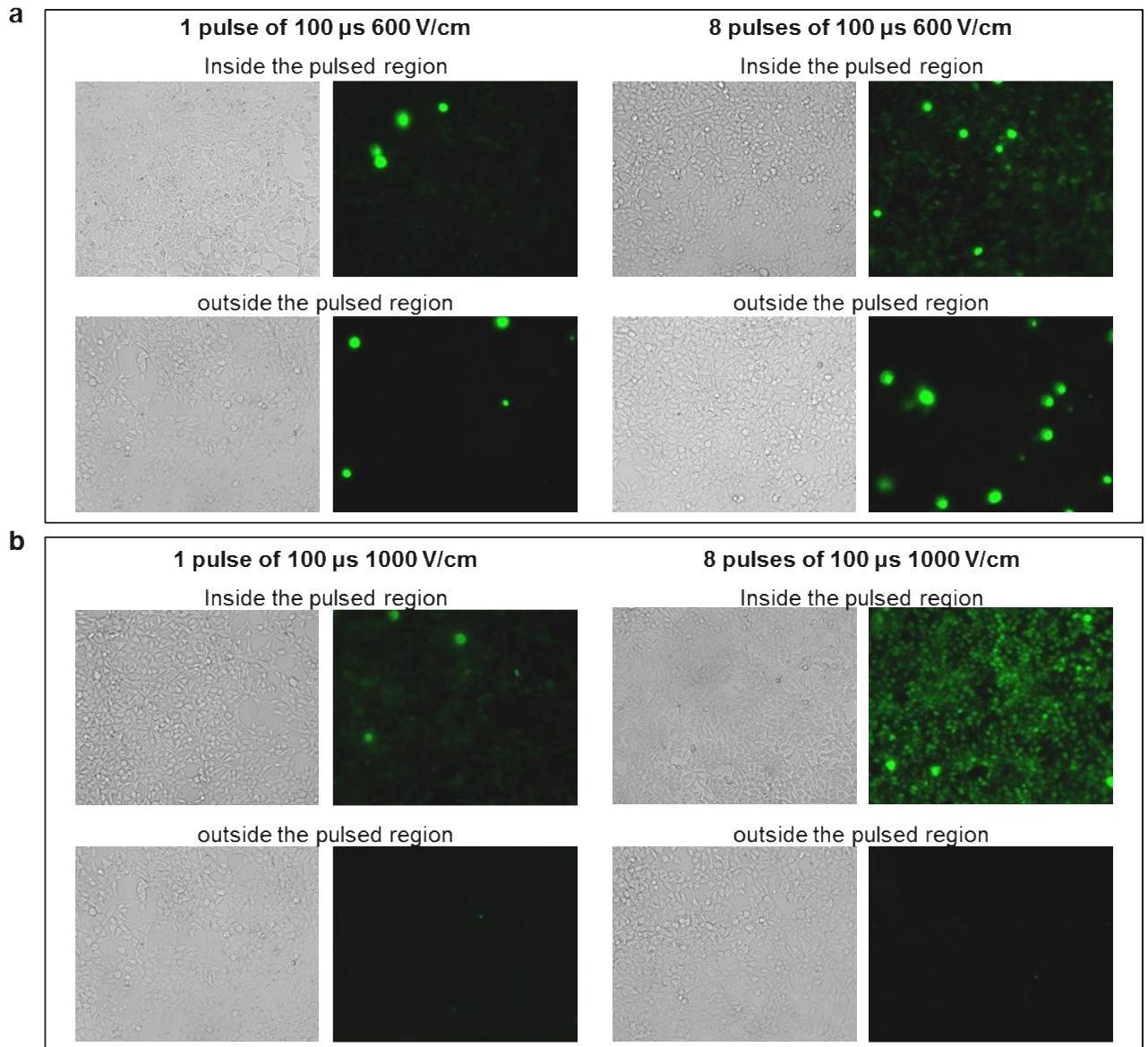
3.3. Pulsed electric fields affect immediate early genes expression

Since the energy density used in the previous section was not able to induce any biological response in terms of redox balance, cell death induction and microRNA expression modulation, higher energy densities were applied to the neuroblastoma cells, by delivering microsecond and nanosecond electric pulses of higher field intensities, in order to explore if any of the above-mentioned biological effects could be induced.

These higher doses were a single electric pulse of 100 μ s, at three different field intensities (10, 600 and 1000 V/cm) or one electric pulse of 10 ns at 1000 V/cm.

We first assessed if these more intense electric pulse conditions were able to permeabilize the cell membrane using YO-PRO-1, a small-molecule fluorescent indicator of membrane integrity. Just after pulse application, a weak intracellular stain was visible when a single 100 μ s pulse at 600 V/cm was applied (Supp Fig. 1A). The fluorescence

was more evident when a single 100 μ s pulse at 1000 V/cm was applied. YO-PRO-1 signal very much increased when 8 repeated 600 or 1000 V/cm were applied, demonstrating a complete and strong permeabilization of the samples. No YO-PRO-1 staining was detected in cells exposed to a single 10 ns pulse at 1000 V/cm. Adherent cells, located in the areas of the cell layer not exposed to the pulses, were negative for the stain (Supp. Fig. 1B).



Supplementary figure 1 YO-PRO-1 staining after the delivery of pulses lasting 100 μ s with an intensity of 600 V/cm (A) and 1000 V/cm (B). YO-PRO-1 uptake after a single pulse and 8 repeated electric pulses at 1 Hz is shown in the left and right panels of the figure, respectively. All images were collected with an exposure time of 300 milliseconds

Finally, in order to assess the immediate molecular cell response to the electric pulses in all the analyzed conditions (both low and high intensities), the expression of two immediate early genes, *c-fos* and *egr-1* (*early growth response protein 1*), was evaluated in cells, up to 6 hours after the exposure. As displayed in Fig. 4, all the different pulse protocols were able to induce a significant increase in *egr-1* expression, which reached its highest level at 1 hour after the exposure, while at 6 hours the *egr-1* expression was comparable or significantly lower than in the not-pulsed controls.

c-fos was significantly increased 1 hour post stimulation for all the pulse exposure conditions, except for the lowest microsecond pulse exposure amplitude (0.1 V/cm). Six hours after the pulse application, *c-fos* mRNA level was again comparable or significantly lower than in the unexposed controls (Fig. 4).

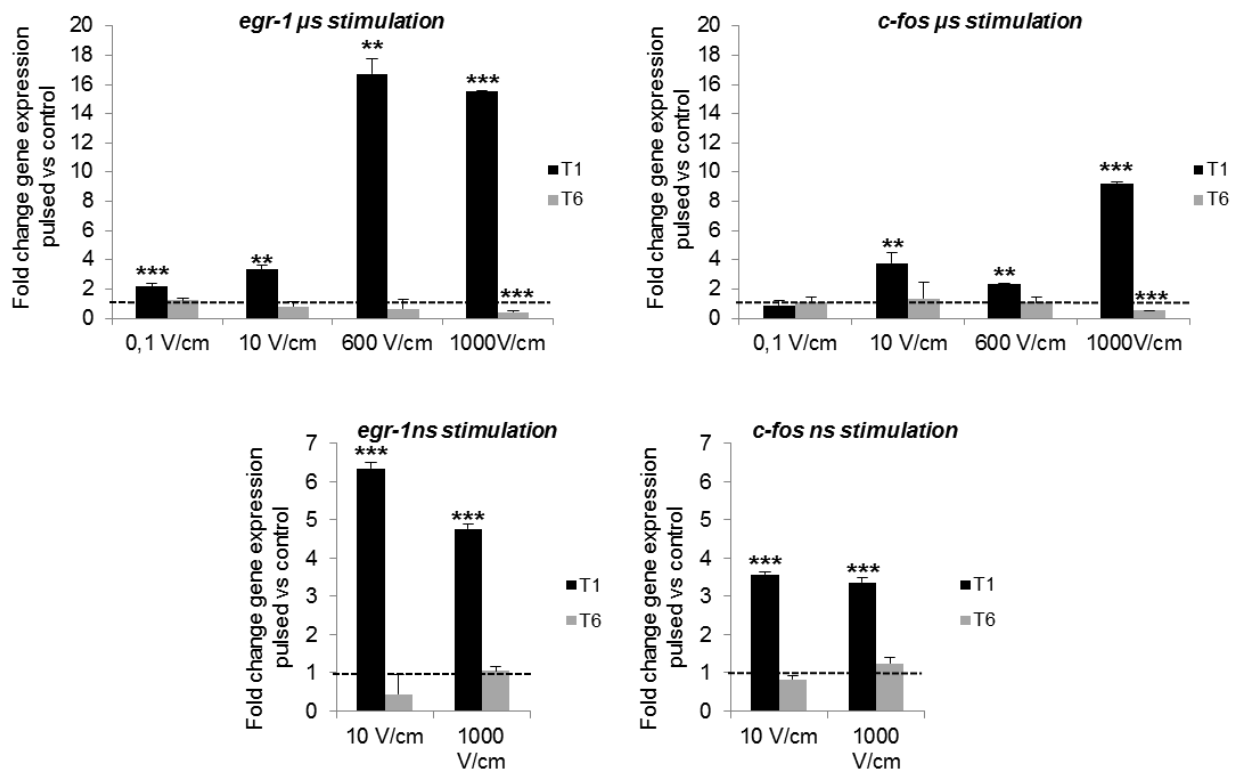


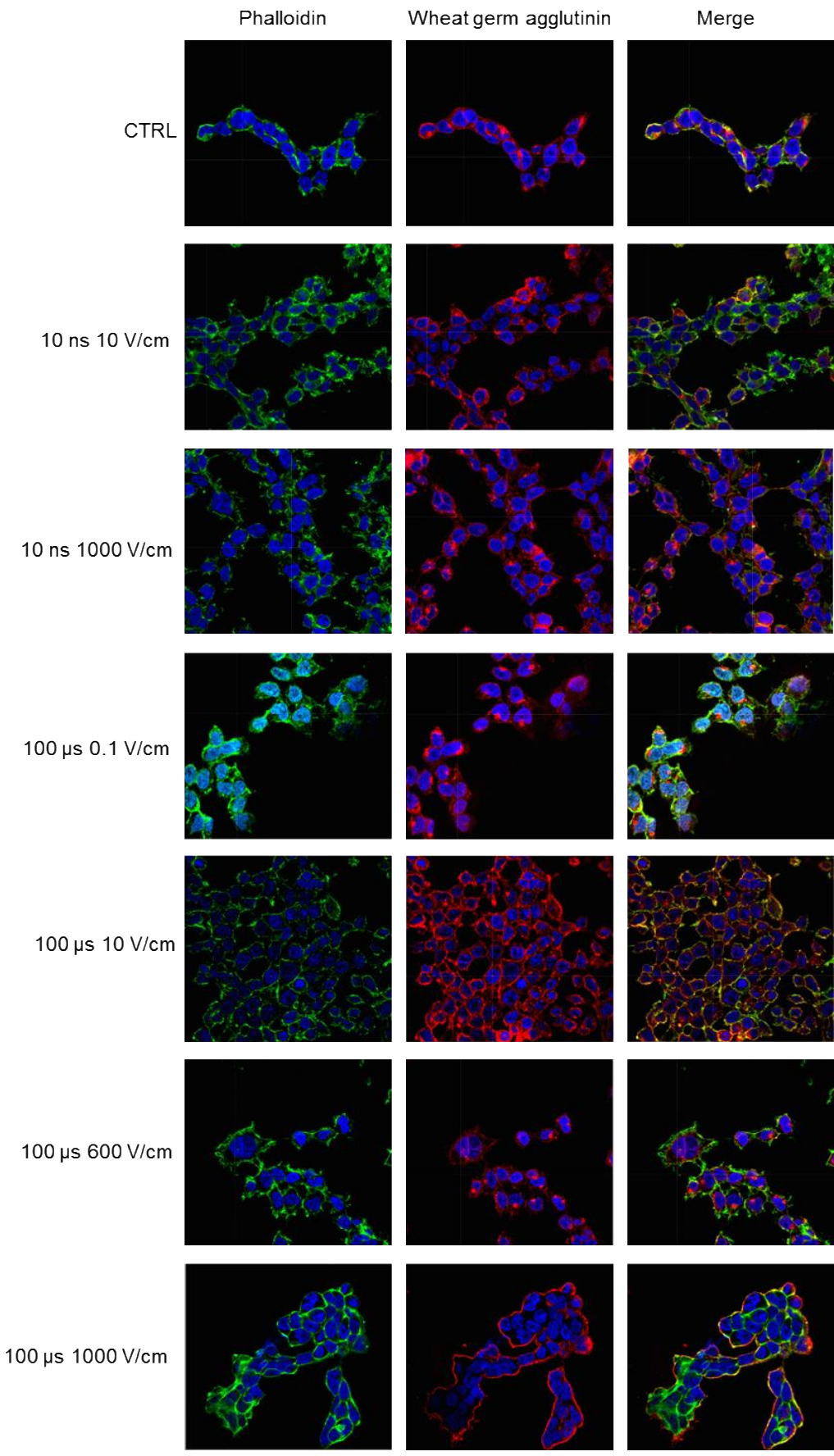
Fig. 4 *egr-1* and *c-fos* expression carried out in the six first hours after the exposure of the cells, under all the pulse conditions. The values are means±SD and represent the fold change in the pulsed samples related to the control (non-pulsed), considered as 1. **P ≤0.05, ***P ≤0.001. The dashed line corresponds to a fold change of 1. Values are the means ± S.D. of three independent experiments

3.4. One pulse, 100 μs, 1000 V/cm exposure induces cell membranes fusion and affects cell morphology

Looking at the cells 24 hour after the exposure to the highest energy density condition, we identified some cells which, viewed with phase contrast microscope, appeared fused (data not shown). For this reason, we investigated whether our conditions of pulse stimulation could effectively induce cell fusion.

We evaluated the cells morphology 24 hour after exposure for all pulse conditions. Cells were examined with fluorescence microscopy after staining with fluorescence derivative of wheat germ agglutinin, which binds to glycoproteins of the cell membrane, and phalloidin, a probe for filamentous actin. Cells stimulated with nanosecond pulses did not show any change in morphology compared to the non-pulsed samples (CTRL, Fig. 5). Among the microsecond pulse exposures, only at the highest pulse intensity, 1000 V/cm, we did observe formation of giant cells with fused membranes, and in these cells the cytoskeleton did not merge (Fig. 5, 100 μs, 1000 V/cm).

1
2
3
4
5
6
7
8
9
10
11
12
13
14
15
16
17
18
19
20
21
22
23
24
25
26
27
28
29
30
31
32
33
34
35
36
37
38
39
40
41
42
43
44
45
46
47
48
49
50
51
52
53
54
55
56
57
58
59
60
61
62
63
64
65



1 **Fig. 5** Confocal fluorescence microscopy images of SH-SY5Y cells pulsed under all the different conditions and stained
2 24 hour later for membrane (with wheat germ agglutinin, in red), actin F (with alexa fluor, in green) and DNA (with
3 DAPI, in blue)
4

5
6 *3.5. Short electric pulses at larger energy densities do not affect redox homeostasis, cell apoptosis or miR-34b and miR*
7 *34c expression*
8
9

10 To investigate whether exposure conditions higher than 100 μ s, 0.1V and 10 ns, 10 V could influence redox
11 homeostasis, ROS production was also evaluated under these exposure conditions, just after the pulse application (T0)
12 and 1, 6, and 24 hour after it.
13
14

15 With nanosecond exposures (10 ns, 1000 V), we observed no variation in ROS production (data not shown). When
16 microsecond pulses were applied, no ROS modulation was observed at T0, T1, and T24 (data not shown). At T6, only
17 at the highest amplitude, a small, not statistically significant, increase in ROS generation was seen (Fig. 6).
18
19

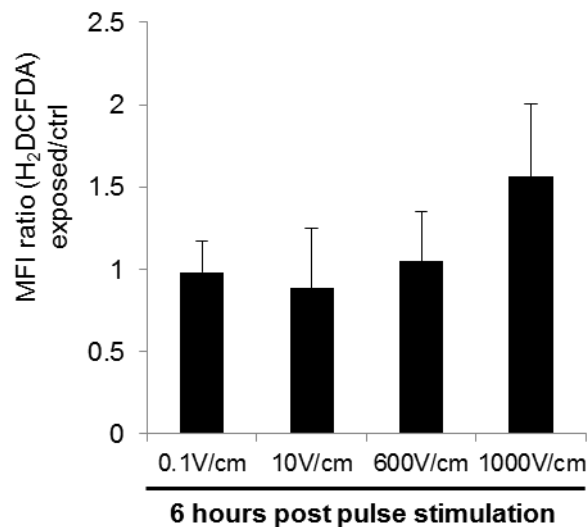


Fig. 6 ROS production assessment 6 hours after one 100 μ s electric pulse at various field amplitudes. ROS were evaluated using the H₂DCFDA probe. Values are the means \pm S.D. of three independent experiments

Since nanosecond and microsecond pulses applied at the same energy condition as that associated with 50 Hz, 1 mT magnetic field exposures did not activate cell apoptosis, we investigated whether higher energy density conditions could promote such an effect. Analyzing PARP-1 cleavage 24 and 48 hours after exposure of cells to these electric pulses, we observed no apoptotic signal for all the different exposure conditions considered (Fig. 7), even for the strongest one that led to a complete cell permeabilization (i.e., 1 pulse, 100 μ s, 1000 V/cm).

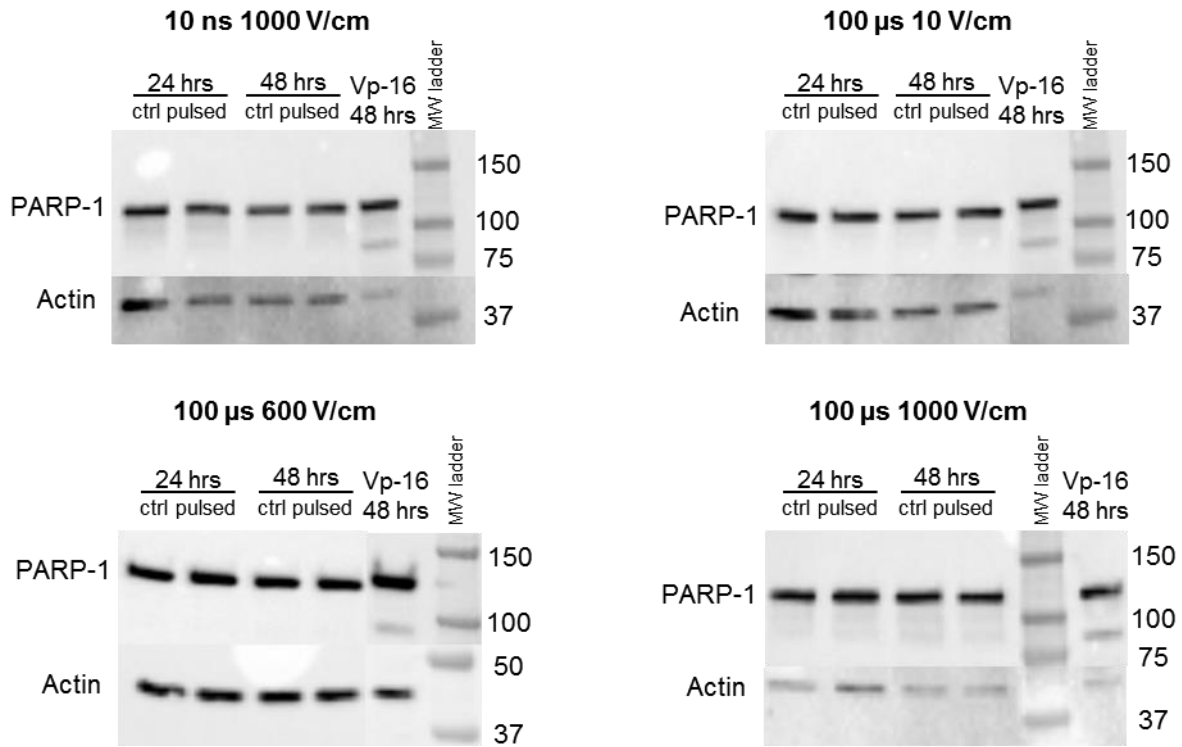
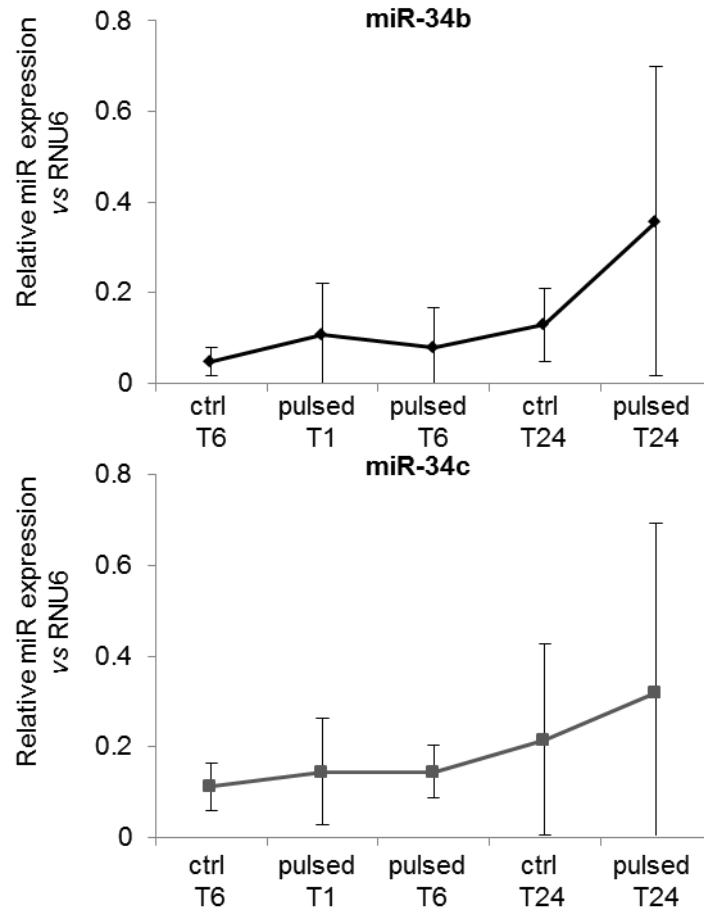


Fig. 7 Cell apoptosis analyzed through western blot analysis of PARP1 cleavage (molecular masses are given in kDa on the right), carried out in SH-SY5Y cells 24 and 48 hours after the exposure to one single electric pulse (conditions reported in the figure). As positive controls, the proteins from cells treated with 5 μ M etoposide for 48 hours were included among the experimental samples. The immunoblots are representative of different experiments giving similar results. Values are the means \pm S.D. of three independent experiments

We also estimated miR-34b and miR-34c expression in cells exposed to one pulse of 100 μ s, 1000 V/cm at 1, 6 and 24 hour after the exposure. Such exposure condition is the strongest used in our experiments. Also, in this case no significant modulation of both microRNAs was detectable (Supp. Fig. 2).



Supplementary figure 2 miR-34b and miR-34c expression evaluated in SH-SY5Y cells at 1 (pulsed T1), 6 (pulsed T6) and 24 (pulsed T24) hours after the cell exposure to one electric pulse of 100 μ s at 1000 V/cm

Discussion

4.1. Role of the energy density and of the electric field amplitude

Despite the large number of *in vitro* and *in vivo* experimental studies focused on the effects of ELF-MF exposure, the specific interaction mechanisms underlying such effects, at the cellular and molecular levels, have not been elucidated so far. Several studies have demonstrated that ELF-MFs can modulate cell redox homeostasis [2, 6, 42], but the modalities for triggering such effects are still a matter of debate.

Unraveling how ELF-MFs interact with biological systems has a fundamental importance both for environmental and occupational safety and for the development of new applications. As widely reported, there is a broad public concern about the spread of electromagnetic field sources in the environment and a possible association between ELF-MF exposure and cancer. These fields were classified in the group 2B, “possibly carcinogenic to humans”, by the International Agency for Research on Cancer (IARC) in 2002 [43]. Up to date, no experimental data supported this hypothesis. On the other hand, both low and high frequency EMF are increasingly being applied in the field of biomedical therapies, with protocols that have arisen from experience only, without the benefit of optimization guided by a predictive theory. Understanding which component of these fields is responsible for the observed effects and what are the underlying molecular pathways would surely lead to improvements in therapeutic efficacy and likely inspire new applications.

We have previously demonstrated that long-term exposure to a 1mT sinusoidal (50Hz) MF affects the redox homeostasis of SH-SY5Y cells by increasing ROS production and depleting the cell antioxidant reserve, which makes the cells more sensitive to the pro-oxidant neurotoxin MPP⁺. Furthermore, 24 and 48 hours of such an exposure induces a decrease in expression of both miR-34b and miR-34c [10, 12]. miR-34b/c share the same promoter [14], and in our experiments we showed that the down-regulation of these two microRNAs was p53-independent and due to another epigenetic event, the hyper-methylation of their promoter.

In the present work, starting from our findings regarding redox balance and epigenome modulation in the neuroblastoma cell line SH-SY5Y following a 50 Hz, 1 mT exposure, we report on the biological effects -on the same cell line- induced by nanosecond or microsecond electric pulses with dose parameters selected to deliver the same energy density as 24 hour, 50 hz, 1 mT magnetic field exposure studied previously [10, 11, 12]. We applied electric pulses lasting either 100 μ s, (a standard pulse length in electrochemotherapy protocols), or 10 ns, because they are among the shortest electric pulses that can be commercially generated and they are potential modality for further clinical applications [21, 22].

The rationale for including nanosecond and microsecond electric pulses in this study came also from curiosity about unexplored biological responses induced by this kind of stimulation. The effects of pulsed electric fields on biological cells and tissues have been studied for more than forty years [44, 45], and it has been established that the most common outcome of these exposures is modification of the plasma membrane, making it more permeable to molecules which, otherwise, cannot cross this barrier [17, 46, 47]. Electric pulses of sufficient magnitude and duration induce a transmembrane potential (TMP), that causes nanoscale rearrangements of the membrane. If the applied field is not too intense and does not last too long, the membrane becomes transiently permeable, without affecting cell viability [48].

The ability of nanosecond and microsecond electric pulses to modify the permeability of the plasma membrane is routinely used in cell biology to transfer DNA into cells [19]. Furthermore, their application enables an effective cancer therapy, electrochemotherapy, by increasing anticancer drugs penetration into tumor cells [17]. Cellular modifications

1 induced by microsecond and nanosecond electric pulses under the electroporation threshold dose, however, have not
2 been clearly identified and characterized. A deeper understanding of cellular responses to both magnetic fields and
3 electric pulses would greatly enhance the range of their application in therapeutics.

4 To compare the biological effects induced by microsecond and nanosecond electric pulses with those observed after
5 exposing SH-SY5Y to a 50 Hz, 1 mT magnetic field, we focused on three biological targets: redox homeostasis, cell
6 viability, and microRNA expression modulation. In our previous work, we observed that an ELF-MF exposure can
7 affect redox balance and miR-34 b/c expression, but contributes to the induction of apoptosis only when the magnetic
8 field is applied before MPP⁺ neurotoxin administration [10].

9 Here, we demonstrate that exposure to a single 10 ns at 10 V/cm pulse or a single 100 μ s 0.1 V/cm pulse, with
10 energy densities equivalent to that during 24 hour, 50 Hz, 1 mT magnetic field, does not affect redox homeostasis in
11 SH-SY5Y cells at any of the considered time points (from T0, just after the pulse application, up to 24 hour after the
12 exposure). Furthermore, these pulses do not induce cell death and do not affect miR-34 b/c expression, which is
13 downregulated in SH-SY5Y cells exposed to a 50 Hz, 1 mT magnetic field [12]. Delivery of a certain DED is,
14 therefore, not sufficient to produce the responses seen after the EMF-MF exposure.

15 One important exposure aspect to be considered is the duration of the exposure itself. The effects detailed in [10, 11]
16 were obtained for exposures lasting at least 24 hour, while nanosecond and microsecond electric pulse delivery with the
17 same DED lasts only 10 ns and 100 μ s, respectively, a duration which could be too short to promote a sustained cell
18 response both in terms of oxidative stress or epigenetic modulation.

19 Another possible contributing factor is the electric field induced by the magnetic field exposure (Faraday's Law). To
20 investigate the possible electric field involvement, we exposed SH-SY5Y cells to a sinusoidal 50 Hz electric field of the
21 same intensity as that induced by 50 Hz, 1 mT magnetic field. No modulation of ROS production was detected,
22 indicating that the magnetically induced electric field is not responsible for the biological effects elicited by the 50 Hz
23 ELF-MF exposure, and suggests that time-varying magnetic field is the possible causative agent.

24 *4.2. Nanosecond and microsecond pulsed electric fields and immediate early genes (IEG) expression*

25 We then explored the effects induced by the delivery of nanosecond and microsecond electric pulses at higher
26 energy densities, up to the dose that results in plasma membrane poration. To search for the molecular responses that
27 are activated by these intermediate-dose electric pulse exposures, where the field amplitude is lower or at the limit of
28 the threshold for the cell membrane permeabilization achievement, cells were exposed to one single pulse at increasing
29 electric field amplitudes up to 1000 V/cm, corresponding to an energy density of 1.5×10^6 J/m³. This is the energy
30 density at which membrane poration becomes clearly evident in our SH-SY5Y cell model.

31 To identify an immediate molecular response induced by these pulses on SH-SY5Y cells, the expression of two
32 IEG, *c-fos* and *egr-1*, was measured 1 and 6 hours after the pulses delivery. IEGs can be activated and transcribed
33 within minutes after stimulation, even in the presence of protein synthesis inhibitors, and they are stimulated in response
34 to both cell-extrinsic and cell-intrinsic signals, in particular to stress. IEG expression is usually quick and transient, and
35 protein products are usually unstable and quickly degraded without ubiquitination. IEGs usually code for transcription
36 factors which then can activate secondary response genes [49].

37 Both Egr-1 and c-Fos are transcription factors which can be activated by a plethora of stimuli [49]. In the nervous
38 system, their expression is restricted to the brain, where they modulate synaptic plasticity and neurite outgrowth [50-
39 52]. Electrical stimuli are able to induce the activation of these two genes. In particular, continuous electrical

1 stimulation of neuronal and neuron-like cells was demonstrated to increase neurite outgrowth through the up-regulation
2 of both transcription factors [53-55].

3 Under our experimental conditions, there was a clear stimulation of IEG expression. *egr-1* expression was
4 statistically up-regulated 1 hour after exposure for all conditions of the applied pulsed electric field, using microsecond
5 or nanosecond pulses, even for the lowest applied DED. At 6 hours *egr-1* expression returned to the basal level, or to
6 levels significantly lower. *c-fos* transcript displayed a similar statistically significant up-regulation, except when cells
7 were pulsed at the lowest energy (i.e. 100 μ s, 0.1 V/cm).
8
9

10 It is very interesting to notice that, for the same energy transferred to the sample, the two pulse conditions 100 μ s at
11 0.1 V/cm and 10 ns at 10 V/cm, produce two different patterns of *c-fos* expression. This leads to the hypothesis that
12 modulation of *c-fos* expression by pulsed electric fields is independent of the DED. We can speculate that these two
13 exposure modalities (microsecond and nanosecond electric pulses) elicit different bio-responses because nanosecond
14 electric pulses have bioelectrical properties different from microsecond ones, such as intracellular penetration and larger
15 electric field amplitude, on top of their duration. [56]. It is worth pointing out that, since the cells were not
16 electroporated by these pulse doses, the differences in the responses to microsecond and nanosecond pulses cannot be
17 accounted for by different modes of permeabilization.
18
19
20
21

22 Our findings demonstrate that the cells respond to an ultrashort electric stimulation below the electroporation
23 threshold. IEG activation in SH-SY5Y cells under, these two stimulation conditions, has not previously investigated, so
24 our results cannot be directly compared to any of the studies conducted so far [25-28, 33, 34]. Both *egr-1* and *c-fos* can
25 be activated by an elevation of intracellular calcium [57, 58], in particular after cell depolarization, when voltage-
26 dependent calcium channels are activated [57, 59]. It seems possible then that, for observations reported here, even
27 when nanosecond and microsecond electric pulses are applied below the electroporation threshold in SH-SY5Y cells,
28 calcium channels could be activated, leading to IEG up-regulation.
29
30
31
32
33

34 4.3. Nanosecond and microsecond pulsed electric fields and cell morphology

35
36
37 A well-known effect induced by nanosecond and microsecond pulses is cell fusion [31, 60-62]. The ability of
38 electric pulses to induce membrane fusion has led to applications like hybridoma formation [63], where this technique is
39 more effective and less toxic than standard methods [64]. For electrofusion to occur, cells need to be in contact and in a
40 “fusogenic state” (related to “electropermeabilized state”), which can be achieved by electric pulses application; this
41 fusogenic state involves a fractural rearrangement of the lipidic bilayer that is similar to that caused by electroporation
42 [65].
43
44
45
46

47 In some of our experiments, we observed cell fusion in samples monitored with phase contrast microscopy. We
48 investigated this phenomenon further, under all the different exposure conditions, by staining cells 24 hour post
49 exposure with a fluorescent marker specific for Actin F (phalloidin) and another for cell membrane (wheat germ
50 agglutinin). We saw changes only in the cells pulsed at the highest energy condition (one pulse of 100 μ s at 1000
51 V/cm): in that case, some giant cells with fused membranes, but separate cytoskeleton, were observed.
52
53

54 Together with other aspects, such as the importance of membrane poration, the membrane fusogenic state, the
55 temperature, and the ionic component of the medium in which cells were pulsed, the involvement of the actin/tubulin
56 cytoskeleton rearrangement and cell swelling during cells electrofusion was demonstrated [66-68]. In SH-SY5Y cells,
57 looking at actin organization, we did not observe its remodeling in fused cells, even though we detected cell swelling,
58
59
60
61
62

1 still clearly visible 24 hour after exposure, when cells were plated at high cell density (more than 70% of confluence;
2 data not shown).

3 Several features differentiate our experimental conditions from the ones described before, and from other studies
4 published in the literature: 1) our highest pulsed electric field condition was lower than the ones usually applied in the
5 other studies; 2) most of the published papers analyzed the biological effects only during the first hours after the pulses
6 delivery; 3) we pulsed cells in cell growth medium (DMEM/F12) which is rich of ions, in particular Ca⁺⁺, which have
7 been demonstrated to play a critical role in guiding electrofusion; 4) we pulsed SH-SY5Y cells which, to the best of our
8 knowledge, have never been used before to investigate nanosecond and microsecond electric pulses effects. This is a
9 crucial point, since the response to these pulses and the ability of the cells to fuse are strictly cell type dependent [31,
10 60].

11 As mentioned before, one of the conditions to trigger fusion is that electroporation occurs. Both the extent of
12 electroporation and the fusion level, can be controlled by the amplitude, duration, and number of the applied pulses;
13 namely, increasing any of the mentioned pulse parameters leads to a higher level of membrane electroporation and
14 consequently higher number of fused cells, if reversible electroporation is assured [31, 69]. Interestingly, in our
15 experiments, cell fusion was observed only at the pulse condition able to electroporate cells. Despite that, it is worth to
16 remember that the energy applied to the bio-samples was very low, probably one of the lowest ever applied in the
17 literature, which demonstrates that also mild electric pulses exposure can induce cell fusion. This aspect could also be
18 related to the specifically used cell line, the SH-SY5Y cells, a neuroblastoma cell line largely used in literature for its
19 neuronal like features [70], which also make this cell line particularly sensitive to calcium fluxes [71], one of the
20 principal actors of the electrofusion [72, 73].

31 *4.4. Nanosecond and microsecond pulsed electric fields and ROS generation, apoptosis, and microRNA*

32 Since with the lowest energy conditions we did not observe redox homeostasis imbalance, apoptosis or miR-34b/c
33 modulation, as previously reported in 50 Hz-exposed cells, we also investigated whether more intense exposure
34 conditions could impact one or several of these parameters. Looking at cell apoptosis none of the conditions considered
35 in our study was able to induce cell death. Similarly, redox homeostasis was not influenced after the cell exposure to
36 any of the analyzed conditions, even though at the highest DED, a slight increase, not statistically significant, in ROS
37 production was observed just after the pulse delivery (T0) and up to 6 hours after the exposure.

38 After nanosecond and microsecond pulse application, ROS production, associated to phospholipids oxidation [23],
39 has been demonstrated, when a specific electric field intensity threshold is reached and plasma membrane is
40 permeabilized [74]. It is important to highlight that, to observe cytoplasmic ROS increase, the electropermeabilization
41 needs to occur and to be reversible, in order to maintain the cell survival [32]. Under our experimental conditions, after
42 the delivery of one 100 μ s electric pulse, cells started to be permeabilized only at 1000 V/cm, confirming that our
43 exposure conditions were much weaker than the ones described in the papers cited before.

44 Even under this electrical stimulation condition, delivering the highest DED in our study, no change in miR-34b/c
45 expression was observed. We can conclude that the expression of these two miRNAs is probably not a target of the
46 electric pulses stimulation, only of the magnetic stimulation [12], or that the experimental conditions used here to
47 deliver the electric pulses were not able to induce a significant change in miR-34b/c expression.

5. Conclusion

The present *in vitro* study tackles the open question related to the role of the DED and the contribution of the induced electric field component to provoke different biological effects observed under or after cells exposure to ELF-MFs.

Responses of SH-SY5Y cells were analyzed after pulsed electric fields at a DED equal to the one delivered by a continuous 24 hour EMF-MF treatment (50 Hz, 1 mT) and also after exposure to a continuous, sinusoidal *electric* field of the same intensity as the one *induced* by the ELF *magnetic* field exposure. None of the tested electric field exposures impaired cellular redox homeostasis, nor did they affect the down-regulation of the miR-34 b/c expression observed following ELF-MF exposure. We can, therefore conclude that neither total DED (delivered from pulsed electric fields instead of a continuous magnetic field) nor the induced electric field associated with the magnetic field exposure are responsible for the biological effects reported in [10-12]. Other components of the ELF-MF exposure that might be considered crucial for the induction of a biological response, such as a direct action of the magnetic field on cells, or the amplitude and the duration of the delivered electric pulses, must be investigated in order to identify the mechanisms of ELF-MFs mediated bio-effects.

It is also important to note that the exploration of the biological effects induced by the pulsed electric fields of different durations and intensities below or at the threshold of cell electroporation on the SH-SY5Y cells revealed the ability of the non-porating electric fields to induce the cell signal transduction through the stimulation of the expression of two immediate early genes (*egr-1* and *c-fos*). Because this stimulation was achieved with no membrane permeabilization, no change in cells morphology and in cell survival, no other apparent perturbation, our results should motivate further studies to disclose possible molecular mechanisms activated by electric pulses exposure, for translation towards new therapeutic and technological applications.

Acknowledgments

1 This research was undertaken during a Short Term Scientific Mission funded within the framework of COST Action
2 EMF-MED (COST Action BM1309), supported by COST (European Cooperation in Science and Technology)
3 Programme. The funding support of CNRS, Université Paris-Saclay and Gustave Roussy is also acknowledged. The
4 work was also partially supported by H2020 MSCA-IF OPTIC BIOEM GA-661041.
5
6

7 We are especially grateful to Professor Tom Vernier for the thorough revision of English and the critical reading of
8 the manuscript.
9

10 We also want to thank Francesca Pacchierotti for her helpful critical review of the manuscript.
11
12
13
14
15
16
17
18
19
20
21
22
23
24
25
26
27
28
29
30
31
32
33
34
35
36
37
38
39
40
41
42
43
44
45
46
47
48
49
50
51
52
53
54
55
56
57
58
59
60
61
62
63
64
65

References

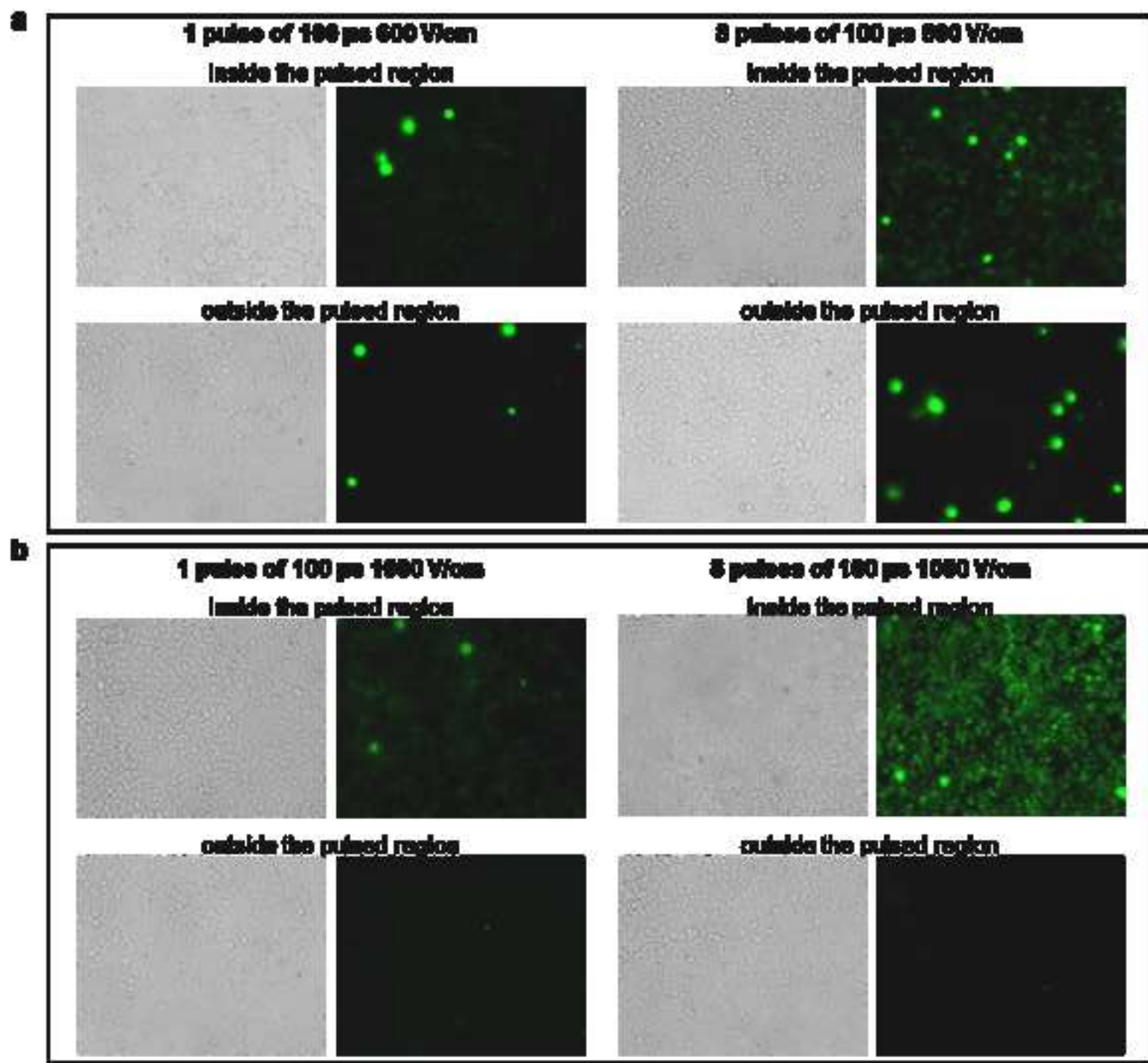
1. Belyaev I, Dean A, Eger H, Hubmann G, Jandrisovits R, Kern M, Kundi M, Moshhammer H, Lercher P, Müller K, Oberfeld G, Ohnsorge P, Pelzmann P, Scheingraber C, Thill R (2016). EUROPAEM EMF Guideline 2016 for the prevention, diagnosis and treatment of EMF-related health problems and illnesses. *Rev Environ Health* 31(3):363-397. doi: 10.1515/reveh-2016-0011.
2. Saliev T, Begimbetova D, Masoud AR, Matkarimov B (2019) Biological effects of non-ionizing electromagnetic fields: Two sides of a coin. *Prog Biophys Mol Biol* 141:25-36. doi: 10.1016/j.pbiomolbio.2018.07.009.
3. Kim JH, Lee JK, Kim HG, Kim KB, Kim H (2019) Possible Effects of Radiofrequency Electromagnetic Field Exposure on Central Nerve System. *Biomol Ther (Seoul)* 27(3):265-275. doi: 10.4062/biomolther.2018.152.
4. Gherardini L, Ciuti G, Tognarelli S, Cinti C (2014) Searching for the perfect wave: the effect of radiofrequency electromagnetic fields on cells. *Int J Mol Sci* 15(4):5366-5387. doi: 10.3390/ijms15045366.
5. Simkó M, Remondini D, Zeni O, Scarfi M (2016) Quality Matters: Systematic Analysis of Endpoints Related to "Cellular Life" in Vitro Data of Radiofrequency Electromagnetic Field Exposure. *Int J Environ Res Public Health* 13(7): pii E701. doi: 10.3390/ijerph13070701.
6. Consales C, Merla C, Marino C, Benassi B (2012) Electromagnetic fields, oxidative stress, and neurodegeneration. *Int J Cell Biol* 2012:683897
7. Di Lazzaro V, Capone F, Apollonio F, Borea PA, Cadossi R, Fassina L, Grassi C, Liberti M, Paffi A, Parazzini M, Varani K, Ravazzani P (2013) A consensus panel review of central nervous system effects of the exposure to low-intensity extremely low-frequency magnetic fields. *Brain Stimul* 6(4):469-476. doi: 10.1016/j.brs.2013.01.004.
8. Consales C, Merla C, Marino C, Benassi B (2018) The epigenetic component of the brain response to electromagnetic stimulation in Parkinson's Disease patients: A literature overview. *Bioelectromagnetics* 39(1):3-14 a. doi: 10.1002/bem.22083.
9. Manikonda PK, Rajendra P, Devendranath D, Gunasekaran B, Channakeshava, Aradhya SR, Sashidhar RB, Subramanyam C (2014) Extremely low frequency magnetic fields induce oxidative stress in rat brain. *Gen Physiol Biophys* 33(1):81-90. doi: 10.4149/gpb_2013059.
10. Benassi B, Filomeni G, Montagna C, Merla C, Lopresto V, Pinto R, Marino C, Consales C (2016) Extremely Low Frequency Magnetic Field (ELF-MF) Exposure Sensitizes SH-SY5Y Cells to the Pro-Parkinson's Disease Toxin MPP+. *Mol Neurobiol* 53(6):4247-4260. doi: 10.1007/s12035-015-9354-4.
11. Merla C, Liberti M, Consales C, Denzi A, Apollonio F, Marino C, Benassi B (2019) Evidences of plasma membrane-mediated ROS generation upon ELF exposure in neuroblastoma cells supported by a computational multiscale approach. *Biochim Biophys Acta Biomembr* 1861(8):1446-1457. doi: 10.1016/j.bbamem.2019.06.005.
12. Consales C, Cirotti C, Filomeni G, Panatta M, Butera A, Merla C, Lopresto V, Pinto R, Marino C, Benassi B (2018) Fifty-Hertz Magnetic Field Affects the Epigenetic Modulation of the miR-34b/c in Neuronal Cells. *Mol Neurobiol* 55(7):5698-5714 b. doi: 10.1007/s12035-017-0791-0.
13. Mohr AM, Mott JL (2015) Overview of microRNA biology. *Semin Liver Dis* 35(1):3-11. doi: 10.1055/s-0034-1397344.
14. Hermeking H (2010) The miR-34 family in cancer and apoptosis. *Cell Death Differ* 17(2):193-9. doi: 10.1038/cdd.2009.56.

15. Wu J, Bao J, Kim M, Yuan S, Tang C, Zheng H, Mastick GS, Xu C, Yan W (2014) Two miRNA clusters, miR-34b/c and miR-449, are essential for normal brain development, motile ciliogenesis, and spermatogenesis. *Proc Natl Acad Sci U S A*. 111(28):E2851-7. doi: 10.1073/pnas.1407777111.
16. Rokavec M, Li H, Jiang L, Hermeking H (2010) The p53/miR-34 axis in development and disease. *J Mol Cell Biol* 6(3):214-30. doi: 10.1093/jmcb/mju003.
17. Breton M, Mir LM (2012) Microsecond and nanosecond electric pulses in cancer treatments. *Bioelectromagnetics* 33(2):106-123. doi: 10.1002/bem.20692.
18. Gehl J, Sersa G, Matthiessen LW, Muir T, Soden D, Occhini A, Quaglino P, Curatolo P, Campana LG, Kunte C, Clover AJP, Bertino G, Farricha V, Odili J, Dahlstrom K, Benazzo M, Mir LM (2018) Updated standard operating procedures for electrochemotherapy of cutaneous tumours and skin metastases. *Acta Oncol* 57(7):874-882. doi: 10.1080/0284186X.2018.1454602.
19. Mir LM (2009) Nucleic acids electrotransfer-based gene therapy (electrogenotherapy): past, current, and future. *Mol Biotechnol* 43(2):167-176. doi: 10.1007/s12033-009-9192-6.
20. Jiang C, Davalos RV, Bischof JC (2015) A review of basic to clinical studies of irreversible electroporation therapy. *IEEE Trans Biomed Eng* 62(1):4-20.
21. Casciola M, Xiao S, Pakhomov AG (2017) Damage-free peripheral nerve stimulation by 12-ns pulsed electric field. *Sci Rep* 7(1):10453. doi: 10.1038/s41598-017-10282-5.
22. Nuccitelli R, McDaniel A, Anand S, Cha J, Mallon Z, Berridge JC, Uecker D (2017) Nano-Pulse Stimulation is a physical modality that can trigger immunogenic tumor cell death. *J Immunother Cancer* 5:32. doi: 10.1186/s40425-017-0234-5.
23. Breton M, Mir LM (2018) Investigation of the chemical mechanisms involved in the electropulsation of membranes at the molecular level. *Bioelectrochemistry* 119:76-83. doi: 10.1016/j.bioelechem.2017.09.005.
24. Vernier PT, Sun Y, Gundersen MA (2006) Nanoelectropulse-driven membrane perturbation and small molecule permeabilization. *BMC Cell Biol* 7:37.
25. Beebe SJ, Chen X, Liu JA, Schoenbach KH (2011) Nanosecond pulsed electric field ablation of hepatocellular carcinoma. *Conf Proc IEEE Eng Med Biol Soc* 2011:6861-6865. doi: 10.1109/IEMBS.2011.6091692.
26. Pakhomova ON, Gregory BW, Semenov I, Pakhomov AG (2013) Two modes of cell death caused by exposure to nanosecond pulsed electric field. *PLoS One* 8(7):e70278. doi: 10.1371/journal.pone.0070278
27. Hanna H, Denzi A, Liberti M, André FM, Mir LM (2017) Electroporation of Inner and Outer Cell Membranes with Microsecond Pulsed Electric Fields: Quantitative Study with Calcium Ions. *Sci Rep* 7(1):13079. doi: 10.1038/s41598-017-12960-w.
28. de Menorval MA, Andre FM, Silve A, Dalmay C, François O, Le Pioufle B, Mir LM (2016) Electric pulses: a flexible tool to manipulate cytosolic calcium concentrations and generate spontaneous-like calcium oscillations in mesenchymal stem cells. *Sci Rep* 6:32331. doi: 10.1038/srep32331.
29. Hristov K, Mangalanathan U, Casciola M, Pakhomova ON, Pakhomov AG (2018) Expression of voltage-gated calcium channels augments cell susceptibility to membrane disruption by nanosecond pulsed electric field. *Biochim Biophys Acta Biomembr* 1860(11):2175-2183. doi: 10.1016/j.bbamem.2018.08.017.
30. Yoon J, Leblanc N, Zaklit J, Vernier PT, Chatterjee I, Craviso GL (2016) Enhanced Monitoring of Nanosecond Electric Pulse-Evoked Membrane Conductance Changes in Whole-Cell Patch Clamp Experiments. *J Membr Biol* 249(5):633-644.

- 1
2
3
4
5
6
7
8
9
10
11
12
13
14
15
16
17
18
19
20
21
22
23
24
25
26
27
28
29
30
31
32
33
34
35
36
37
38
39
40
41
42
43
44
45
46
47
48
49
50
51
52
53
54
55
56
57
58
59
60
61
62
63
64
65
31. Salomskaite-Davalgiene S, Cepurniene K, Satkauskas S, Venslauskas MS, Mir LM (2009) Extent of cell electrofusion in vitro and in vivo is cell line dependent. *Anticancer Res* (8):3125-3130.
 32. Bonnafous P, Vernhes M, Teissié J, Gabriel B (1999) The generation of reactive-oxygen species associated with long-lasting pulse-induced electropermeabilisation of mammalian cells is based on a non-destructive alteration of the plasma membrane. *Biochim Biophys Acta* 1461(1):123-134.
 33. Pakhomova ON, Khorokhorina VA, Bowman AM, Rodaitė-Riševičienė R, Saulis G, Xiao S, Pakhomov AG (2012) Oxidative effects of nanosecond pulsed electric field exposure in cells and cell-free media. *Arch Biochem Biophys* 527(1):55-64. doi: 10.1016/j.abb.2012.08.004
 34. Pakhomov AG, Bowman AM, Ibey BL, Andre FM, Pakhomova ON, Schoenbach KH (2009) Lipid nanopores can form a stable, ion channel-like conduction pathway in cell membrane. *Biochem Biophys Res Commun* 385(2):181-186. doi: 10.1016/j.bbrc.2009.05.035.
 35. Sano MB, Arena CB, DeWitt MR, Saur D, Davalos RV (2014) In-vitro Bipolar Nano- And Microsecond Electro-Pulse Bursts for Irreversible Electroporation Therapies. *Bioelectrochemistry* 100:69-79. doi: 10.1016/j.bioelechem.2014.07.010.
 36. Ibey BL, Pakhomov AG, Gregory BW, Khorokhorina VA, Roth CC, Rassokhin MA, Bernhard JA, Wilmink GJ, Pakhomova ON (2010) Selective cytotoxicity of intense nanosecond-duration electric pulses in mammalian cells. *Biochim Biophys Acta* 1800(11):1210-1219. doi: 10.1016/j.bbagen.2010.07.008.
 37. Maček-Lebar A, Miklavčič D (2001) Cell electropermeabilization to small molecules in vitro: control by pulse parameters. *Radiol Oncol* 35(3):193-202
 38. Schoenbach KH, Joshi RP, Beebe SJ, Baum CE (2009) A scaling law for membrane permeabilization with nanopulses. *IEEE Transactions on Dielectrics and Electrical Insulation* 16(5): 1224-1235. doi: 10.1109/TDEI.2009.5293932.
 39. Merla C, El Amari S, Kanaan M, liberti M, Apollonio F, Arnaud-Cormos D, Couderc C, Leveque P (2010) A 10- High-Voltage Nanosecond Pulse Generator. *IEEE TMTT* 58(12): 4079-4085.
 40. Silve A, Vezinet R, Mir L (2012) Nanosecond-Duration Electric Pulse Delivery In Vitro and In Vivo: Experimental Considerations. *IEEE TIM* 61(7): 1945-1954.
 41. Livak KJ, Schmittgen TD (2001) Analysis of relative gene expression data using real-time quantitative PCR and the 2(-Delta Delta C(T)) Method. *Methods* 25(4):402-408.
 42. Kivrak EG, Yurt KK, Kaplan AA, Alkan I, Altun G (2017) Effects of electromagnetic fields exposure on the antioxidant defense system. *J Microsc Ultrastruct* 5(4):167-176. doi: 10.1016/j.jmau.2017.07.003.
 43. International Agency for Research on Cancer-(IARC) (2002). Nonionizing radiation Part I: static and extremely low frequency (ELF) electric and magnetic fields. *Monographs* 80:1-429.
 44. Sher LD, Kresch E, Schwan HP (1970) On the possibility of nonthermal biological effects of pulsed electromagnetic radiation. *Biophys J* 10(10):970-9.
 45. Farndale RW, Maroudas A, Marsland TP (1987) Effects of low-amplitude pulsed magnetic fields on cellular ion transport. *Bioelectromagnetics* 8(2):119-134.
 46. Joshi RP, Schoenbach KH (2010) Bioelectric effects of intense ultrashort pulses. *Crit Rev Biomed Eng* 38(3):255-304.
 47. Batista Napotnik T, Reberšek M, Vernier PT, Mali B, Miklavčič D (2010) Effects of high voltage nanosecond electric pulses on eukaryotic cells (in vitro): A systematic review. *Bioelectrochemistry* 110:1-12. doi: 10.1016/j.bioelechem.2016.02.011.

- 1
2
3
4
5
6
7
8
9
10
11
12
13
14
15
16
17
18
19
20
21
22
23
24
25
26
27
28
29
30
31
32
33
34
35
36
37
38
39
40
41
42
43
44
45
46
47
48
49
50
51
52
53
54
55
56
57
58
59
60
61
62
63
64
65
48. Teissie J (2014) Electroporation of the cell membrane. *Methods Mol Biol* 1121:25-46. doi: 10.1007/978-1-4614-9632-8_2.
 49. Bahrami S, Drabløs F (2016) Gene regulation in the immediate-early response process. *Adv Biol Regul* 62:37-49. doi: 10.1016/j.jbior.2016.05.001.
 50. Duclot F, Kabbaj M (2017) The Role of Early Growth Response 1 (EGR-1) in Brain Plasticity and Neuropsychiatric Disorders. *Front Behav Neurosci* 11:35. doi: 10.3389/fnbeh.2017.00035.
 51. Okuno H (2011) Regulation and function of immediate-early genes in the brain: beyond neuronal activity markers. *Neurosci Res* 69(3):175-86. doi: 10.1016/j.neures.2010.12.007.
 52. Jaworski J, Kalita K, Knapska E (2018) c-Fos and neuronal plasticity: the aftermath of Kaczmarek's theory. *Acta Neurobiol Exp (Wars)* 78(4):287-296.
 53. Yan X, Liu J, Huang J, Huang M, He F, Ye Z, Xiao W, Hu X, Luo Z (2014) Electrical stimulation induces calcium-dependent neurite outgrowth and immediate early genes expressions of dorsal root ganglion neurons. *Neurochem Res* 39(1):129-41. doi: 10.1007/s11064-013-1197-7.
 54. Fields RD (1994) Regulation of neurite outgrowth and immediate early gene expression by patterned electrical stimulation. *Prog Brain Res* 103:127-36.
 55. Chang YJ, Hsu CM, Lin CH, Lu MS, Chen L (2013) Electrical stimulation promotes nerve growth factor-induced neurite outgrowth and signaling. *Biochim Biophys Acta*. 1830(8):4130-6. doi: 10.1016/j.bbagen.2013.04.007.
 56. Nuccitelli R (2019) Application of pulsed electric fields to cancer therapy. *Bioelectricity* 1(1):30-34. <https://doi.org/10.1089/bioe.2018.0001>
 57. Thiel G, Mayer SI, Müller I, Stefano L, Rössler OG (2010) Egr-1-A Ca(2+)-regulated transcription factor. *Cell Calcium* 47(5):397-403. doi:10.1016/j.ceca.2010.02.005
 58. Morgan JI, Curran T (1986) Role of ion flux in the control of c-fos expression *Nature* 322(6079):552-5.
 59. Sheng M, McFadden G, Greenberg ME (1990) Membrane depolarization and calcium induce c-fos transcription via phosphorylation of transcription factor CREB. *Neuron* 4(4):571-82
 60. Mekid H, Mir LM (2000) In vivo cell electrofusion. *Biochim Biophys Acta* 1524(2-3):118-30.
 61. Rems L, Ušaj M, Kandušer M, Reberšek M, Miklavčič D, Pucihar G (2013) Cell electrofusion using nanosecond electric pulses. *Sci Rep* 3:3382. doi: 10.1038/srep03382.
 62. Li C, Ke Q, Yao C, Mi Y, Liu H, Lv Y, Yao C (2018) Cell electrofusion based on nanosecond/microsecond pulsed electric fields. *PLoS One* 13(5):e0197167. doi: 10.1371/journal.pone.0197167.
 63. Ke Q, Li C, Wu M, Ge L, Yao C, Yao C, Mi Y (2019) Electrofusion by a bipolar pulsed electric field: Increased cell fusion efficiency for monoclonal antibody production. *Bioelectrochemistry* 127:171-179. doi: 10.1016/j.bioelechem.2019.02.007.
 64. Ishizaki K, Chang HR, Eguchi T, Ikenaga M (1989) High voltage electric pulses efficiently induce fusion of cells in monolayer culture. *Cell Struct Funct* 14(2):173-81.
 65. Teissie J, Rols MP (1986) Fusion of mammalian cells in culture is obtained by creating the contact between cells after their electroporation. *Biochem Biophys Res Commun* 140(1):258-66.
 66. Kandušer M, Ušaj M (2014) Cell electrofusion: past and future perspectives for antibody production and cancer cell vaccines. *Expert Opin Drug Deliv* 11(12):1885-98. doi: 10.1517/17425247.2014.938632.
 67. Blangero C, Rols MP, Teissie J (1989) Cytoskeletal reorganization during electric-field-induced fusion of Chinese hamster ovary cells grown in monolayers. *Biochim Biophys Acta* 981(2):295-302.

- 1
2
3
4
5
6
7
8
9
10
11
12
13
14
15
16
17
18
19
20
21
22
23
24
25
26
27
28
29
30
31
32
33
34
35
36
37
38
39
40
41
42
43
44
45
46
47
48
49
50
51
52
53
54
55
56
57
58
59
60
61
62
63
64
65
68. Meulenberg CJ, Todorovic V, Cemazar M (2012) Differential cellular effects of electroporation and electrochemotherapy in monolayers of human microvascular endothelial cells. *PLoS One* 7(12):e52713. doi: 10.1371/journal.pone.0052713.
 69. Teissié J, Ramos C (1998) Correlation between electric field pulse induced long-lived permeabilization and fusogenicity in cell membranes. *Biophys J* 74(4):1889-98.
 70. Kovalevich J, Langford D (2013) Considerations for the use of SH-SY5Y neuroblastoma cells in neurobiology. *Methods Mol Biol* 1078:9-21. doi: 10.1007/978-1-62703-640-5_2.
 71. Lambert DG, Nahorski SR (1990) Second-messenger responses associated with stimulation of neuronal muscarinic receptors expressed by a human neuroblastoma SH-SY5Y. *Prog Brain Res* 84:31-42. doi: 10.1016/s0079-6123(08)60886-9.
 72. Ohnishi K, Chiba J, Goto Y, Tokunaga T (1987) Improvement in the basic technology of electrofusion for generation of antibody-producing hybridomas. *J Immunol Methods* 100(1-2):181-9.
 73. Suo L, Wang F, Zhou GB, Shi JM, Wang YB, Zeng SM, Tian JH, Zhu SE, Liu GS (2009) Optimal concentration of calcium and electric field levels improve tetraploid embryo production by electrofusion in mice. *J Reprod Dev* 55(4):383-5.
 74. Gabriel B, Teissié J (1994) Generation of reactive-oxygen species induced by electropermeabilization of Chinese hamster ovary cells and their consequence on cell viability. *Eur J Biochem* 223(1):25-33.



gimp suppl fig 1.tif

